Highly Pathogenic Avian Influenza A(H5N8) Clade 2.3.4.4b Viruses in Satellite-Tracked Wild Ducks, Ningxia, China, 2020

Xinru Lv,[1] Xiang Li,[1] Heting Sun,[1] Yi Li,[1] Peng Peng, Siyuan Qin, Weidong Wang, Yuecheng Li, Qing An, Tian Fu, Fengyi Qu, Qiuzi Xu, Rongxiu Qin, Zhenliang Zhao, Meixi Wang, Yulong Wang, Yajun Wang, Xiangwei Zeng, Zhijun Hou, Chengliang Lei, Dong Chu, Yanbing Li, Hongliang Chai

During October 2020, we identified 13 highly pathogenic avian influenza A(H5N8) clade 2.3.4.4b viruses from wild ducks in Ningxia, China. These viruses were genetically related to H5N8 viruses circulating mainly in poultry in Europe during early 2020. We also determined movements of H5N8 virus–infected wild ducks and evidence for spreading of viruses.

A novel reassortant highly pathogenic avian influenza (HPAI) A(H5N8) virus belonging to clade 2.3.4.4 was detected in poultry and wild birds in South Korea during January 2014 (*1*) and spread rapidly by migration of wild birds to Asia, Europe, and North America (*2*). Clade 2.3.4.4 HPAI H5N8 viruses caused additional influenza outbreaks worldwide during 2016 and continued circulating in birds in Asia, Europe, and Africa (*3*–*5*).

In October 2020, clade 2.3.4.4b HPAI H5N8 viruses were detected in wild swans in China (*6*). A clade 2.3.4.4b H5N8 virus infection in humans was reported in Russia during December 2020, indicating a possible increased risk for these viruses crossing species barriers (*7*). In this study, we investigated the emergence of HPAI H5N8 viruses in wild ducks in Ningxia, in western China, during October 2020 and performed satellite tracking to determine the flyways of wild ducks.

Author affiliations: Northeast Forestry University College of Wildlife and Protected Area, Harbin, China (X. Lv, X. Li, Yi Li, Q. An, T. Fu, F. Qu, Q. Xu, R. Qin, Z. Zhao, M. Wang, Yulong Wang, Yajun Wang, X. Zeng, Z. Hou, H. Chai); National Forestry and Grassland Administration, Shenyang, China (H. Sun, P. Peng, S. Qin, C. Lei, D. Chu); Monitoring Center for Terrestrial Wildlife Epidemic Diseases, Yinchuan, China (W. Wang, Yuecheng Li); Harbin Veterinary Research Institute, Harbin (Yanbing Li)

DOI: https://doi.org/10.3201/eid2805.211580

The Study

Ningxia, located at the intersection of the Central Asian and East Asian-Australasian Flyways, is an ideal location for influenza surveillance. We collected 275 paired oropharyngeal and cloacal swab specimens from net-caught wild ducks at the Changshantou Reservoir in Ningxia (37°16′14″N, 105°43′5″E) during October 2020. We inoculated all samples into 10-day-old, embryonated, specific pathogen–free chicken eggs for virus isolation. Thirteen samples were positive for H5N8 subtype avian influenza virus (AIV) by reverse transcription PCR. We sequenced full-length genomes and submitted them to the GISAID EpiFlu database (https://www.gisaid.org) (Appendix Table 1, https://wwwnc.cdc.gov/EID/article/28/5/21-1580-App1.pdf).

We attached solar-powered global positioning system satellite trackers to 12 apparently healthy mallards (*Anas platyrhynchos*) at the capture site and released the birds immediately. We successfully obtained movement tracks for 9 mallards to identify their wintering and stopover sites. We isolated H5N8 viruses from 2 of the satellite-tracked mallards (birds NX-175 and NX-176), but the remaining 7 mallards were negative for AIV (Figure; Appendix Table 2, Figures 1, 2).

All H5N8 isolates were identified as HPAIVs by the amino acid sequence REKRRKR/GLF at the hemagglutinin (HA) cleavage site. H5 phylogenetic analysis classified Ningxia isolates into clade 2.3.4.4b and divided them into 2 distinct groups according to tree topology (Appendix Figure 3). Most isolates (n = 12) shared high nucleotide identities in 8 gene segments (99.6%–100%) with viruses responsible for disease outbreaks in poultry in Europe during early 2020; these segments were closely related to H5N8 viruses

[1]These authors contributed equally to this article

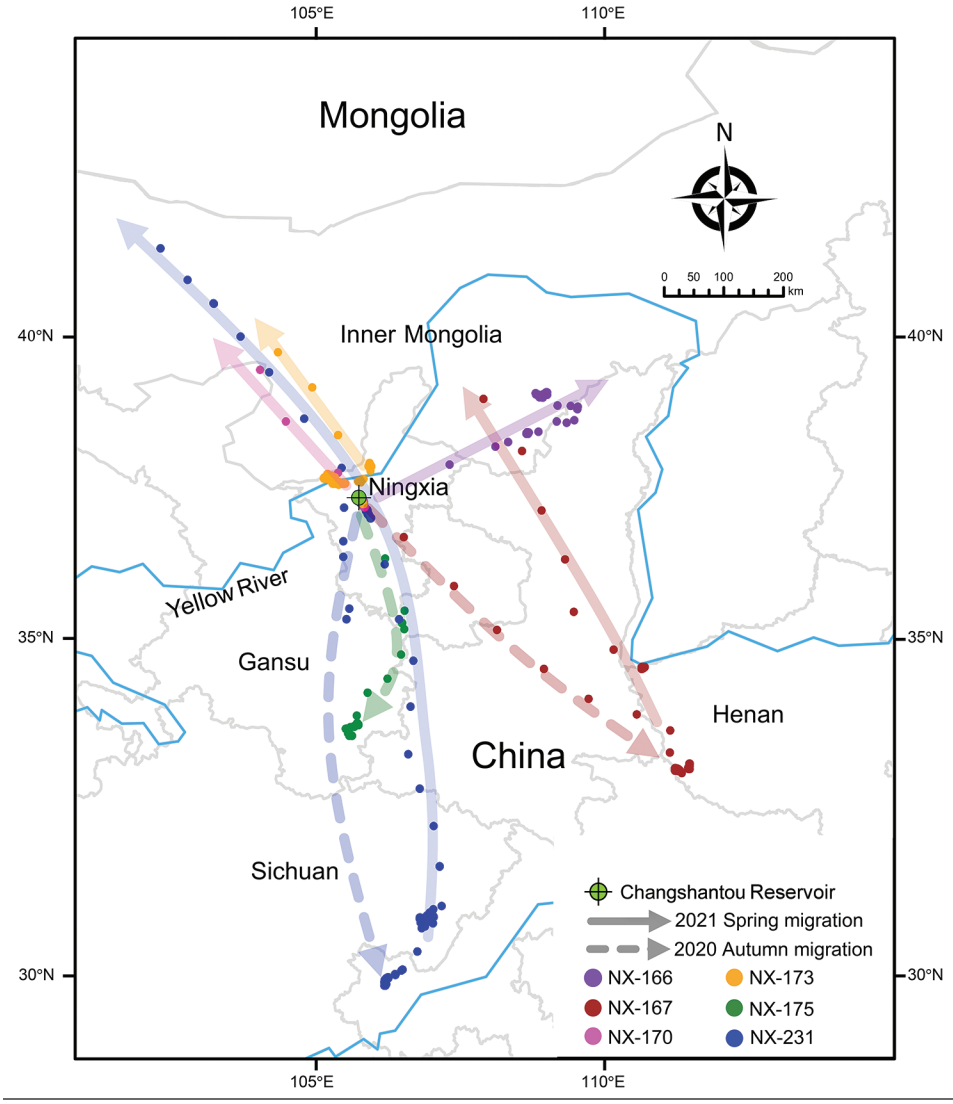

Figure. Migratory routes of 6 of 9 successfully satellite-tracked mallards infected with highly pathogenic avian influenza A(H5N8) clade 2.3.4.4b viruses, Ningxia, China, 2020. Mallards are indicated by different colors. The sampling site (Changshantou Reservoir) is indicated. Solid and dashed lines indicate spring migration in 2021 and autumn migration in 2020, respectively. Because the other 3 successfully satellite-tracked mallards (birds NX-169, NX-174, and NX-176) had been moving around the sampling point, their movements are not shown.

from South Korea and Japan, isolated in October and November 2020 and recognized as subclade 2.3.4.4b1, (Appendix Table 3). The remaining isolate, A/common teal/Ningxia/105/2020(H5N8) (from mallard NX-105), clustered with HPAI H5 viruses that were prevalent in Eurasia in autumn 2020 and recognized as subclade 2.3.4.4b2. A similar tree topology was shown in all 8 segments of Ningxia virus isolates (Appendix Figure 4). Mallard isolate NX-105 and the human isolate A/Astrakhan/3212/2020(H5N8) (human H5N8) from Russia had relatively high nucleotide identities of 99.2%–99.8% in 8 gene segments.

Bayesian phylogenetic analysis showed that the most recent common ancestor of the genome of isolate NX-105 and its neighbor strains emerged during June–October 2020. Ningxia b1 isolates emerged during August–September 2020, and East Asian lineage (b1 viruses including Ningxia subclade 2.3.4.4b1 isolates, strains from Japan and South Korea) emerged at the genome level during May–August 2020 (Appendix Table 4, Figure 5).

Several amino acid mutations in the HA protein (H5 numbering) were associated with increased binding to human-like receptor (α–2,6–sialic acid) (*8*–*11*). Both Ningxia H5N8 isolates and the human H5N8 isolate from Russia had the S133A and T156A mutations, and isolate NX-105 had extra T188I and V210I substitutions, suggesting that this isolate might be more adaptable at infecting humans than the human H5N8 virus. All isolates lacked the Q222L and G224S mutations in the HA protein, including the human H5N8 virus, and lacked the mammalian adaptation markers Q591K, E627K, and D701N mutations in the polymerase basic 2 protein (*12*). Both Ningxia H5N8 isolates and the human H5N8 virus also had other molecular markers associated with

increased virulence and transmission among mammals (Appendix Table 5).

Satellite tracking showed that 2 mallards (NX-167, negative for AIV, and NX-175, infected with H5N8 virus) migrated to the wintering ground without a long duration in Ningxia. Mallard NX-167 flew directly to Henan at a high speed (82.1–116.2 km/h). In contrast, mallard NX-175 showed a greatly decreased speed (34.1–61.8 km/h) after a short stopover at the junction of Ningxia and Gansu, and eventually reached Gansu (Appendix Figure 1). Another H5N8-infected mallard (NX-176) had been moving around the sampling site until we lost the tracking signals on December 25, 2020 (Appendix Figure 2). These results indicated that mallards could continue to migrate after being infected with HPAI H5N8 viruses, but their movements would be affected.

Conclusions

Previous studies have demonstrated a key role for wild waterfowl in the continental transmission of HPAIVs (*13*). In this study, we inferred that H5N8 viruses emerging in Ningxia were likely to be transmitted by migration of infected wild ducks. H5N8 virus outbreaks occurred in the poultry industry in Europe during spring 2020, and the responsible viruses might have been introduced into the wild-bird gene pool through contact with infected poultry (*14*). Wild ducks are short-distance migratory birds, which generally find it difficult to migrate directly from Europe to eastern Asia. Strains from eastern Asia had high nucleotide identity (99.3%–100%) at the genome level, indicating that subclade 2.3.4.4b1 H5N8 viruses might be maintained at common breeding and stopover sites of wild ducks that winter in China, Japan, and South Korea.

The long branch lengths for all segments of the East Asian lineage compared with those for strains from Europe suggested that the virus had been circulating undetected for the intervening period and seemed to have a common ancestor from older viruses during early 2020 or 2019 (Appendix Figure 4). A previous study of the origin of clade 2.3.4.4b HPAI H5N6 viruses isolated in wild ducks in Ningxia in 2017 indicated a similar transmission pattern (*15*). In addition, isolate NX-105 showed an extremely close phylogenetic relationship with the 2020 isolates from Russia (Appendix Figure 4), which also seemed to be transmitted to China by migratory wild ducks.

The movement of mallard NX-175 proved that mallards infected with HPAI H5N8 viruses could continue to migrate, resulting in potential wide spreading of HPAI H5N8 viruses (Appendix Figure 1). Satellite tracking showed that continuous and stable tracking signals for 3 mallards (NX-170, NX-173, and NX-231) migrating northward during April 2021 were suddenly lost during a high-speed flight in Inner Mongolia (Figure). Assuming no damage to the transmitters, we inferred that these 3 mallards had already flown out of China for breeding, and we will therefore not receive additional signals from overseas until the birds return to China during their autumn migration. Further satellite tracking studies are being performed to determine the breeding and stopover grounds in northern Ningxia, China, as essential means of tracing the origins of AIVs and providing future early warnings for these viruses.

Ningxia H5N8 virus isolates showed highly similar mutations to those of human H5N8 viruses, and isolate NX-105 is highly homologous at the genome level, indicating that wild duck–origin viruses could pose an increased threat to public health. Long-term surveillance of wild bird–origin AIVs and international collaboration in AIV monitoring of migratory birds will help support early warning for influenza epidemics.

Acknowledgments

We thank the authors and submitting laboratories for providing sequences to the GISAID EpiFlu Database and International Science Editing (http://www.international-scienceediting.com) for editing the manuscript.

This study was supported by the National Natural Science Foundation of China (grant 31970501) and the National Forestry and Grassland Administration.

About the Author

Ms. Lv is a graduate student at Northeast Forestry University, College of Wildlife and Protected Area, Harbin, China. Her primary research interest is the epidemiology of influenza viruses in wild birds.

References

1. Lee YJ, Kang HM, Lee EK, Song BM, Jeong J, Kwon YK, et al. Novel reassortant influenza A(H5N8) viruses, South Korea, 2014. Emerg Infect Dis. 2014;20:1087–9. https://doi.org/10.3201/eid2006.140233
2. Verhagen JH, Herfst S, Fouchier RA. Infectious disease. How a virus travels the world. Science. 2015;347:616–7. https://doi.org/10.1126/science.aaa6724
3. Li M, Liu H, Bi Y, Sun J, Wong G, Liu D, et al. Highly pathogenic avian influenza A(H5N8) virus in wild migratory birds, Qinghai Lake, China. Emerg Infect Dis. 2017;23:637–41. https://doi.org/10.3201/eid2304.161866
4. Alarcon P, Brouwer A, Venkatesh D, Duncan D, Dovas CI, Georgiades G, et al. Comparison of 2016–17 and previous

epizootics of highly pathogenic avian influenza H5 Guangdong lineage in Europe. Emerg Infect Dis. 2018;24:2270–83. https://doi.org/10.3201/eid2412.171860
5. Selim AA, Erfan AM, Hagag N, Zanaty A, Samir AH, Samy M, et al. Highly pathogenic avian influenza virus (H5N8) clade 2.3.4.4 infection in migratory birds, Egypt. Emerg Infect Dis. 2017;23:1048–51. https://doi.org/10.3201/eid2306.162056
6. Li X, Lv X, Li Y, Peng P, Zhou R, Qin S, et al. Highly pathogenic avian influenza A(H5N8) virus in swans, China, 2020. Emerg Infect Dis. 2021;27:1732–4. https://doi.org/10.3201/eid2706.204727
7. Pyankova OG, Susloparov IM, Moiseeva AA, Kolosova NP, Onkhonova GS, Danilenko AV, et al. Isolation of clade 2.3.4.4b A(H5N8), a highly pathogenic avian influenza virus, from a worker during an outbreak on a poultry farm, Russia, December 2020. Euro Surveill. 2021;26. https://doi.org/10.2807/1560-7917.ES.2021.26.24.2100439
8. Yang ZY, Wei CJ, Kong WP, Wu L, Xu L, Smith DF, et al. Immunization by avian H5 influenza hemagglutinin mutants with altered receptor binding specificity. Science. 2007;317:825–8. https://doi.org/10.1126/science.1135165
9. Wang W, Lu B, Zhou H, Suguitan AL Jr, Cheng X, Subbarao K, et al. Glycosylation at 158N of the hemagglutinin protein and receptor binding specificity synergistically affect the antigenicity and immunogenicity of a live attenuated H5N1 A/Vietnam/1203/2004 vaccine virus in ferrets. J Virol. 2010;84:6570–7. https://doi.org/10.1128/JVI.00221-10
10. Watanabe Y, Ibrahim MS, Ellakany HF, Kawashita N, Mizuike R, Hiramatsu H, et al. Acquisition of human-type receptor binding specificity by new H5N1 influenza virus sublineages during their emergence in birds in Egypt. PLoS Pathog. 2011;7:e1002068. https://doi.org/10.1371/journal.ppat.1002068
11. Chutinimitkul S, van Riel D, Munster VJ, van den Brand JM, Rimmelzwaan GF, Kuiken T, et al. In vitro assessment of attachment pattern and replication efficiency of H5N1 influenza A viruses with altered receptor specificity. J Virol. 2010;84:6825–33. https://doi.org/10.1128/JVI.02737-09
12. Yamada S, Hatta M, Staker BL, Watanabe S, Imai M, Shinya K, et al. Biological and structural characterization of a host-adapting amino acid in influenza virus. PLoS Pathog. 2010;6:e1001034. https://doi.org/10.1371/journal.ppat.1001034
13. Global Consortium for H5N8 and Related Influenza Viruses. Role for migratory wild birds in the global spread of avian influenza H5N8. Science. 2016;354:213–7. https://doi.org/10.1126/science.aaf8852
14. Lewis NS, Banyard AC, Whittard E, Karibayev T, Al Kafagi T, Chvala I, et al. Emergence and spread of novel H5N8, H5N5 and H5N1 clade 2.3.4.4 highly pathogenic avian influenza in 2020. Emerg Microbes Infect. 2021;10:148–51. https://doi.org/10.1080/22221751.2021.1872355
15. Sun J, Zhao L, Li X, Meng W, Chu D, Yang X, et al. Novel H5N6 avian influenza virus reassortants with European H5N8 isolated in migratory birds, China. Transbound Emerg Dis. 2020;67:648–60. https://doi.org/10.1111/tbed.13380

Address for correspondence: Hongliang Chai, Northeast Forestry University, College of Wildlife and Protected Area, NO.26 Hexing Rd, Xiangfang District, Harbin 150040, Heilongjiang, China; email: hongliang_chai@hotmail.com

Article DOI: https://doi.org/10.3201/eid2805.211580

Highly Pathogenic Avian Influenza A(H5N8) Clade 2.3.4.4b Viruses in Satellite-Tracked Wild Ducks, Ningxia, China, 2020

Appendix

Materials and Methods

Samples and Virus Isolation

A total of 275 paired oropharyngeal and cloacal swab specimens were collected from net-caught wild ducks at Changshantou Reservoir, Ningxia, western China (N37°16′14″, E105°43′5″), in October 2020. The samples were oscillated and then centrifuged, and the collected supernatant was inoculated into 10-day-old specific-pathogen-free chicken embryos (National Poultry Laboratory Animal Resource Center, Harbin Veterinary Research Institute, Chinese Academy of Agriculture Sciences, Harbin, China). After 72 hours of incubation, the allantoic fluid was harvested, and the hemagglutinin (HA) activity was assayed. HA-positive isolates were further subtyped by hemagglutinin inhibition and neuraminidase inhibition assays. Viral RNA was extracted from HA-positive allantoic fluid by using QIAamp Viral RNA Mini Kit (QIAGEN, https://www.qiagen.com), reverse transcribed by using the primer Un12 and subjected to reverse transcription PCR by using the method of the World Health Organization.

Genome Sequencing

The PCR products of 8t fragments of the Ningxia H5N8 isolates were sequenced by using a set of specific sequencing primers previously reported (*1*). The sequence data were compiled by using the SeqMan Program (DNASTAR, https://www.dnastar.com). Thirteen H5N8 influenza viruses were isolated from 6 mallards (*Anas platyrhynchos*), 6 common teals (*A. crecca*), and 1 common pochard (*Aythya ferina*). Nucleotide sequences have been deposited in GISAID (https://www.gisaid.org) under accession nos. EPI_ISL_2815336, EPI_ISL_2815374, EPI_ISL_2820250, EPI_ISL_2820259, EPI_ISL_2820261, EPI_ISL_2820262, EPI_ISL_2820288, EPI_ISL_2820465, EPI_ISL_2820479, EPI_ISL_2820480, EPI_ISL_2820501, EPI_ISL_2820503, and EPI_ISL_2820504.

Phylogenetic Analysis

Homologous sequences of the Ningxia H5N8 isolates were obtained by BLAST search at the GISAID Epiflu databases in early January 2021, and 8 datasets were derived from the top 100 BLASTn hits and the genome of clade 2.3.4.4 H5N8 viruses isolated in 2020. Sequences without full alignment length were excluded. Sequences were aligned by using MAFFT (*2*) implemented in PhyloSuite version 1.2.1 (*3*). The maximum-likelihood tree of each gene was estimated by using IQ-TREE (*4*) under the best-fit substitution model for 1,0000 ultrafast bootstraps (*5*). Best-fit substitution model was selected by using the Bayesian information criterion by ModelFinder (*6*) implemented in PhyloSuite 1.21 (*3*).

For estimation of the time to the most recent common ancestor, Bayesian analysis was performed for all 8 gene segments by using BEAST version 1.10.4. (*7*). The best-fit substitution model was chosen as described above. We specified an uncorrelated lognormal relaxed clock and constant size tree prior for each segment (*8,9*). A Markov

chain Monte Carlo method was used with 50 million chain lengths to draw inference under this model. Three independent runs were combined for analyses to ensure that an adequate effective sample size (200). A maximum clade credibility tree with mean height was generated for each dataset by using TreeAnnotator version 1.10.4 (https://beast.community/treeannotator) after 10% burn-in. The maximum clade credibility trees were visualized by using FigTree version 1.4.4 (http://tree.bio.ed.ac.uk).

Satellite Tracking

On October 15 and 16, 2020, apparently healthy mallards among the sampled birds were chosen for the satellite tracking study. We recorded bodyweight, age (adult or juvenile) and sex for each mallard before equipping them with GPS-GSM (Global Positioning System—Global System for Mobile Communications), solar-powered backpack transmitters. All mallards were released at the capture site instantly after equipping. The transmitters were obtained from Hunan Global Messenger Technology Co. Ltd., https://en.hqxs.net), and the model is HQBG1815S (http://www.hqxs.net/). The transmitters weighed 1.4%–1.5% of the mallards' body mass (average 1,032 g). Location data of the GPS transmitters were acquired from the China Mobile Communication System at 1 location in 2 h intervals by using GSM cards and were reported as latitude, longitude, and location time. The accuracy of the GPS transmitters was categorized into 5 classes: A (± 5 m), B (± 10 m), C (± 20 m), D (± 100 m), and E (± 2,000 m), and the positioning accuracy credibility is 95%. We restricted accuracy to A, B, C, and D for our analysis. We identified the wintering and stopover sites by major clusters of sequential position data, which contrasted with consistent movements and high flight speed (km/hr) during migration. This data enabled identification of the arrival and departure dates at the wintering or stopover sites, and we were able to identify the timing and duration of stopovers and migration flights, as well as the distances between stopovers. If the emitted

signals lost for >1 month, it implied that the transmitter-tagged bird was sick or dead, then the flyway monitoring was terminated.

References

1. Chai H. Molecular epidemiological study on influenza virus in wild birds of Heilongjiang [PhD dissertation]. Harbin (China): Northeast Forestry University; 2012.

2. Katoh K, Standley DM. MAFFT multiple sequence alignment software version 7: improvements in performance and usability. Mol Biol Evol. 2013;30:772–80. PubMed https://doi.org/10.1093/molbev/mst010

3. Zhang D, Gao F, Jakovlić I, Zou H, Zhang J, Li WX, et al. PhyloSuite: an integrated and scalable desktop platform for streamlined molecular sequence data management and evolutionary phylogenetics studies. Mol Ecol Resour. 2020;20:348–55. PubMed https://doi.org/10.1111/1755-0998.13096

4. Nguyen LT, Schmidt HA, von Haeseler A, Minh BQ. IQ-TREE: a fast and effective stochastic algorithm for estimating maximum-likelihood phylogenies. Mol Biol Evol. 2015;32:268–74. PubMed https://doi.org/10.1093/molbev/msu300

5. Minh BQ, Nguyen MA, von Haeseler A. Ultrafast approximation for phylogenetic bootstrap. Mol Biol Evol. 2013;30:1188–95. PubMed https://doi.org/10.1093/molbev/mst024

6. Kalyaanamoorthy S, Minh BQ, Wong TK, von Haeseler A, Jermiin LS. ModelFinder: fast model selection for accurate phylogenetic estimates. Nat Methods. 2017;14:587–9. PubMed https://doi.org/10.1038/nmeth.4285

7. Drummond AJ, Rambaut A. BEAST: Bayesian evolutionary analysis by sampling trees. BMC Evol Biol. 2007;7:214. PubMed https://doi.org/10.1186/1471-2148-7-214

8. Drummond AJ, Ho SY, Phillips MJ, Rambaut A. Relaxed phylogenetics and dating with confidence. PLoS Biol. 2006;4:e88. PubMed https://doi.org/10.1371/journal.pbio.0040088

9. Kingman JF. The coalescent. Stochastic Process Appl. 1982;13:235–48. https://doi.org/10.1016/0304-4149(82)90011-4

Appendix Table 1. Information of the thirteen H5N8 viruses isolated in Ningxia, China, October 2020

GISAID accession no.	Isolate name	Collection date	Clade	Abbreviation
EPI_ISL_2815336	A/common teal/Ningxia/105/2020(H5N8)	2020-Oct-11	2.3.4.4b2	NX-105
EPI_ISL_2815374	A/mallard/Ningxia/175/2020(H5N8)	2020-Oct-15	2.3.4.4b1	NX-175
EPI_ISL_2820250	A/mallard/Ningxia/176/2020(H5N8)	2020-Oct-15	2.3.4.4b1	NX-176
EPI_ISL_2820259	A/common teal/Ningxia/181/2020(H5N8)	2020-Oct-15	2.3.4.4b1	NX-181
EPI_ISL_2820261	A/common teal/Ningxia/189/2020(H5N8)	2020-Oct-15	2.3.4.4b1	NX-189
EPI_ISL_2820262	A/common teal/Ningxia/237/2020(H5N8)	2020-Oct-16	2.3.4.4b1	NX-237
EPI_ISL_2820288	A/mallard/Ningxia/239/2020(H5N8)	2020-Oct-16	2.3.4.4b1	NX-239
EPI_ISL_2820465	A/mallard/Ningxia/241/2020(H5N8)	2020-Oct-16	2.3.4.4b1	NX-241
EPI_ISL_2820479	A/common pochard/Ningxia/243/2020(H5N8)	2020-Oct-16	2.3.4.4b1	NX-243
EPI_ISL_2820480	A/common teal/Ningxia/245/2020(H5N8)	2020-Oct-16	2.3.4.4b1	NX-245
EPI_ISL_2820501	A/mallard/Ningxia/247/2020(H5N8)	2020-Oct-16	2.3.4.4b1	NX-247
EPI_ISL_2820503	A/mallard/Ningxia/249/2020(H5N8)	2020-Oct-16	2.3.4.4b1	NX-249
EPI_ISL_2820504	A/common teal/Ningxia/253/2020(H5N8)	2020-Oct-16	2.3.4.4b1	NX-253

Appendix Table 2. Characteristics of 9 mallards (*Anas platyrhynchos*) we successfully satellite tracked and their migration movements up to May 2021

Bird ID	Sex (Age)*	Weight (g)	Equiping date	AIV test result	Wintering site	Arrival date at wintering site	Departure date at wintering site
NX-166	F (A)	1,010	2020-Oct-15	Negative	Ningxia	Before 2020-Oct-15	2021-Mar-31
NX-167	M (A)	1,115	2020-Oct-15	Negative	Henan	2020-Oct-21	2021-Mar-25
NX-169	M (A)	1,050	2020-Oct-15	Negative	Ningxia	Never left Ningxia	
NX-170	M (A)	925	2020-Oct-15	Negative	Ningxia	Before 2020-Oct-15	2021-Apr-22
NX-173	M (A)	1,100	2020-Oct-15	Negative	Ningxia	Before 2020-Oct-15	2021-Apr-7
NX-174	M (A)	1,000	2020-Oct-15	Negative	Ningxia	Never left Ningxia	
NX-175	F (A)	1,060	2020-Oct-15	H5N8	Gansu	2020-Oct-16	
NX-176	M (A)	1,030	2020-Oct-16	H5N8	Ningxia	Never left Ningxia	
NX-231	F (A)	995	2020-Oct-16	Negative	Sichuan	2020-Dec-24	2021-Mar-24

*A, adult; AIV, avian influenza virus.

Appendix Table 3. Information for clade 2.3.4.4b1 isolates in this study

Date	Location	Isolate name	Isolate ID
2020-Oct-21	South Korea	A/Mandarin duck/Korea/H242/2020	EPI_ISL_631824
2020-Oct-24	South Korea	A/Mandarin duck/Korea/K20–551–4/2020	EPI_ISL_666687
2020-Oct-24	Japan	A/northern pintail/Hokkaido/M13/2020	EPI_ISL_697771
2020-Nov-09	Japan	A/environment/Kagoshima/KU-ngr-J2/2020(H5N8)	EPI_ISL_682297
2019-Dec-30	Poland	A/turkey/Poland/23/2019	EPI_ISL_402134
2020-Jan-01	Poland	A/laying_hen/Poland/002/2020	EPI_ISL_525439
2020-Jan-02	Poland	A/chicken/Poland/003/2020	EPI_ISL_525440
2020-Jan-02	Poland	A/chicken/Poland/004/2020	EPI_ISL_525441
2020-Jan-06	Poland	A/hawk/Poland/003/2020	EPI_ISL_405813
2020-Jan-09	Poland	A/turkey/Poland/027/2020	EPI_ISL_525442
2020-Jan-12	Poland	A/domestic_goose/Poland/028/2020	EPI_ISL_525443
2020-Jan-17	Poland	A/chicken/Poland/054/2020	EPI_ISL_525444
2020-Jan-25	Poland	A/turkey/Poland/079/2020	EPI_ISL_525445
2020-Jan-27	Poland	A/laying_hen/Poland/095/2020	EPI_ISL_525446
2020-Jan-28	Poland	A/turkey/Poland/096/2020	EPI_ISL_525447
2020-Feb-20	Poland	A/domestic_duck/Poland/219/2020	EPI_ISL_525449
2020-Feb-20	Poland	A/domestic_duck/Poland/221/2020	EPI_ISL_525450
2020-Feb-21	Poland	A/domestic_duck/Poland/222/2020	EPI_ISL_525451
2020-Mar-01	Poland	A/domestic_goose/Poland/274/2020	EPI_ISL_525462
2020-Jan-16	Germany	A/white-fronted goose/Germany-BB/AI00018/2020(H5N8)	EPI_ISL_404993
2020-Feb-06	Germany	A/chicken/Germany-BW/AI00049/2020	EPI_ISL_410291
2020-Mar-12	Germany	A/chicken/Germany-SN/AI00276/2020	EPI_ISL_415197
2020-Mar-20	Germany	A/buzzard/Germany-SN/AI00285/2020	EPI_ISL_417414
2020-Mar-20	Germany	A/turkey/Germany-NI/AI00334/2020	EPI_ISL_417415
2020-Mar-26	Germany	A/steamer duck/Germany-SN/AI00346/2020	EPI_ISL_419312
2020-Mar-27	Germany	A/turkey/Germany-ST/AI00352/2020	EPI_ISL_419314
2020-Jan-17	Czech Republic	A/chicken/Czech Republic/1175–1/2020	EPI_ISL_405391
2020-Feb-17	Czech Republic	A/turkey/Czech Republic/3071/2020	EPI_ISL_418266
2020-Jan-09	Hungary	A/turkey/Hungary/1020_20VIR749–1/2020	EPI_ISL_419220
2020-Mar-25	Hungary	A/Duck/Hungary/14788/2020	EPI_ISL_780096
2020-Mar-26	Hungary	A/Goose/Hungary/15267/2020	EPI_ISL_796011

Appendix Table 4. Time of the most recent common ancestor of selected node that contained each gene segment of viruses associated with H5N8 viruses isolated in Ningxia, China, October 2020*.

			95% HPD		
Segment	Node†	tMRCA	Earliest date	Latest date	Posterior value
PB2	1	2020 Sep.	2020 Aug.	2020 Sep.	0.9873
	2	2020 Jul.	2020 May.	2020 Sep.	1
	3	2020 Aug.	2020 Jul.	2020 Oct.	0.9989
PB1	1	2020 Jul.	2020 Apr.	2020 Sep.	1
	2	2020 Jul.	2020 May.	2020 Aug.	0.2388
PA	1	2020 Aug.	2020 Jul.	2020 Sep.	1
	2	2020 May.	2020 Feb.	2020 Aug.	1
	3	2020 Aug.	2020 Jul.	2020 Sep.	0.4015
HA	1	2020 Sep.	2020 Jul.	2020 Sep.	1
	2	2020 May.	2020 Feb.	2020 Aug.	1
	3	2020 Jun.	2020 Apr.	2020 Aug.	0.4552
NP	1	2020 Jun.	2020 Mar.	2020 Aug.	1
	2	2020 Aug.	2020 Jul.	2020 Oct.	1
NA	1	2020 Aug.	2020 Jun.	2020 Sep.	0.9702
	2	2020 Jun.	2020 Feb.	2020 Sep.	1
	3	2020 Aug.	2020 Jun.	2020 Oct.	0.5622
M	1	2020 Sep.	2020 Aug.	2020 Oct.	0.9999
	2	2020 Aug.	2020 May.	2020 Sep.	1
	3	2020 Oct.	2020 Aug.	2020 Oct.	0.9767
NS	1	2020 Sep.	2020 Aug.	2020 Oct.	1
	2	2020 Jul.	2020 Apr.	2020 Sep.	1
	3	2020 Sep.	2020 Aug.	2020 Oct.	0.9613

*HPD, highest posterior density; PB2, polymerase basic 2; PB1, polymerase basic 1; PA, polymerase acidic; HA, hemagglutinin; NP, nucleoprotein; M, matrix; NS, nonstructural; tMRCA, time of the most recent common ancestor.

†Nodes marked in the maximum clade credibility phylogenetic trees (Appendix Figure 2).

Appendix Table 5. Molecular characterization of H5N8 viruses isolated in Ningxia, October 2020, and the H5N8 virus that infected humans in Russia, December 2020*

Protein	Position	Ningxia b1 isolates	Ningxia b2 isolate	A/Astrakhan/3212/2020(H5N8)
HA	S133A	+	+	+
(H5 numbering)†	T156A	+	+	+
	T188I	-	+	-
	V210I	-	+	-
	Q222L	-	-	-
	G224S	-	-	-
PB2‡	Q591K	-	-	-
	E627K	-	-	-
	D701N	-	-	-
M1§	N30D	+	+	+
	I43M	+	+	+
	T215A	+	+	+
NS§	P42S	+	+	+
	80–84 deletion	NO	NO	NO
	L98F	+	+	+
	I101M	+	+	+

*HA, hemagglutinin; PB2, polymerase basic 2; M, matrix; NS, nonstructural; Ningxia b1 isolates, the twelve clade 2.3.4.4b1 H5N8 viruses isolated in Ningxia, October 2020; Ningxia b2 isolate, A/common teal/Ningxia/105/2020(H5N8), the clade 2.3.4.4b2 H5N8 virus isolated in Ningxia, October 2020; +, mutation; –, no mutation.

†S133A, T156A, T188I, V210I, Q222L, and G224S mutations in HA have been associated with increased binding to human-like receptor (α-2–6 sialic acid).

‡Q591K, E627K, and D701N mutations have been associated with increased adaptation of avian influenza virus in mammalian host.

§N30D, I43M, T215A, P42S, 80–84 deletion, L98F, and I101M mutations have been associated with increased virulence in mice.

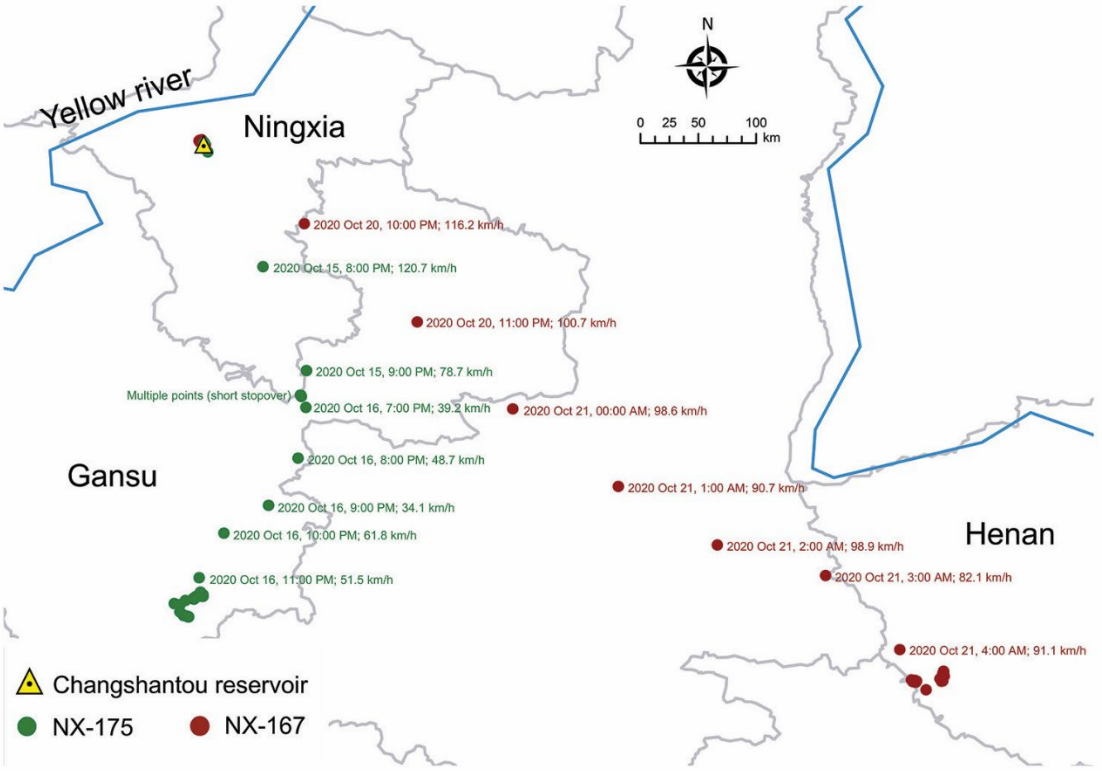

Appendix Figure 1. During October 15–30, 2020, movements of 2 successfully satellite-tracked mallards (*Anas platyrhynchos*). Time and flight speed of every moving point during the migration of the 2 mallards is displayed. The sampling site (Changshantou Reservoir) is indicated.

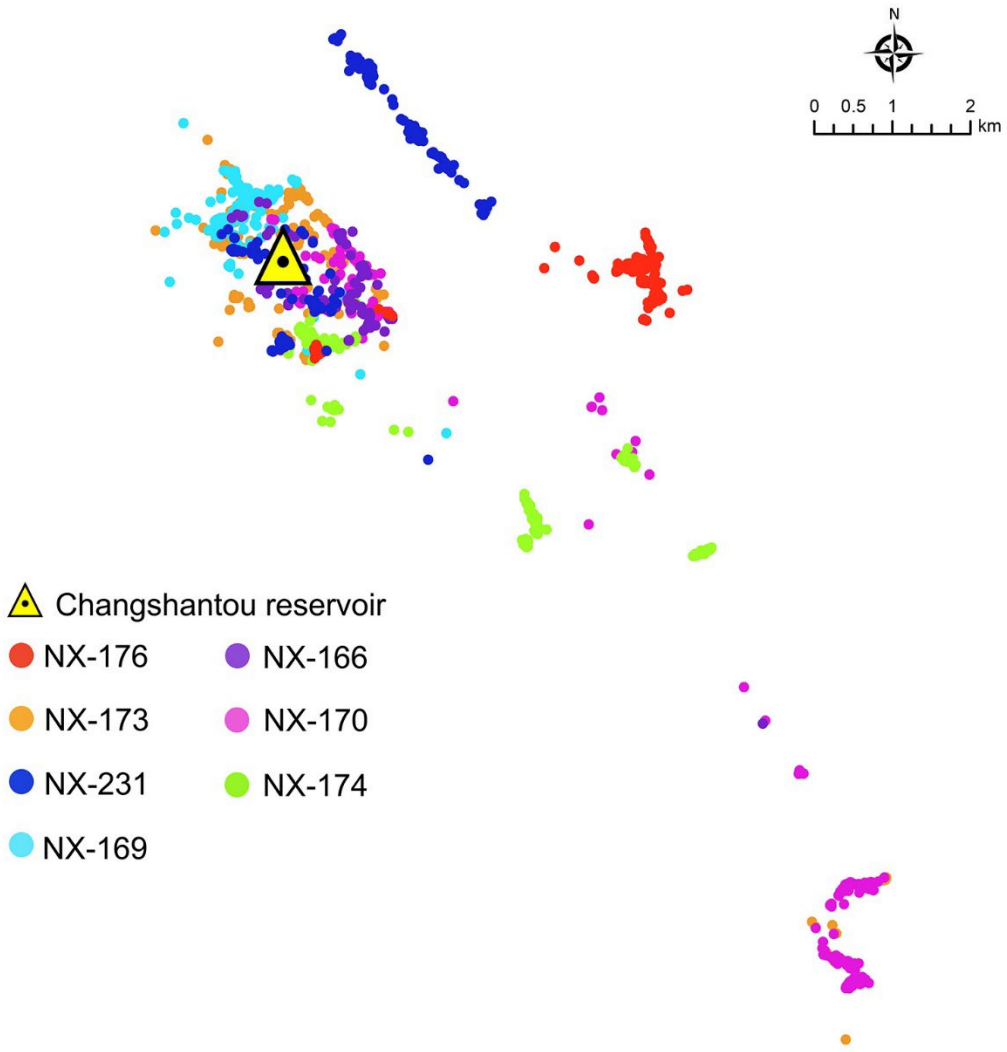

Appendix Figure 2. During October 15–30, 2020, movements of 7 successfully satellite-tracked mallards. Movements are represented by different colors. The sampling site at Changshantou Reservoir is indicated.

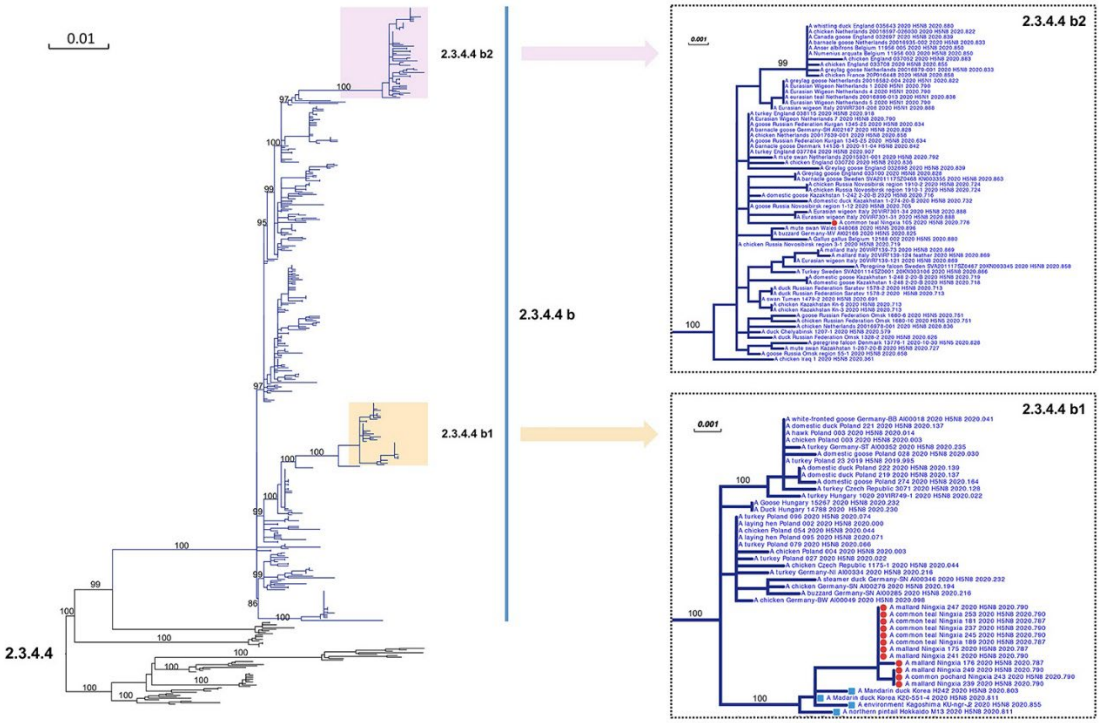

Appendix Figure 3. Maximum-likelihood phylogenetic trees for hemagglutinin genes of avian influenza A(H5N8) viruses isolated in Ningxia, China, 2020, and comparison with clade 2.3.4.4 reference isolates. Dark blue lines indicate viruses that belonged to clade 2.3.4.4b, and black lines indicate viruses that belonged to clade 2.3.4.4a, c–h. Subtrees marked with orange and purple backgrounds indicate subclade 2.3.4.4b1 and subclade 2.3.4.4b2, respectively. The 2 subtrees indicated in the 2 boxes on the right show our Ningxia H5N8 isolates (red circles) and H5N8 viruses isolated from South Korea and Japan during October and November 2020 (blue squares). UFBoot support values of the major branch are indicated. Numbers along branches are bootstrap values. Scale bars indicate nucleotide substitutions per site.

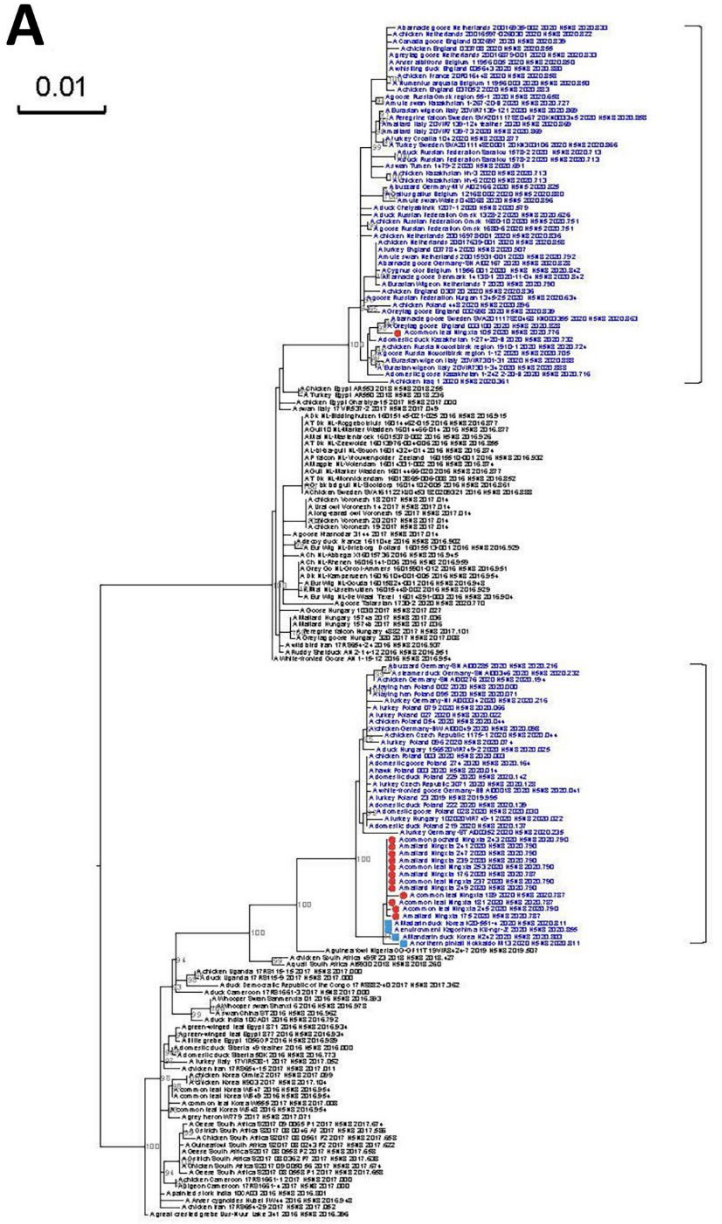
A
0.01
2.3.4.4b2-like
2.3.4.4b1-like

B

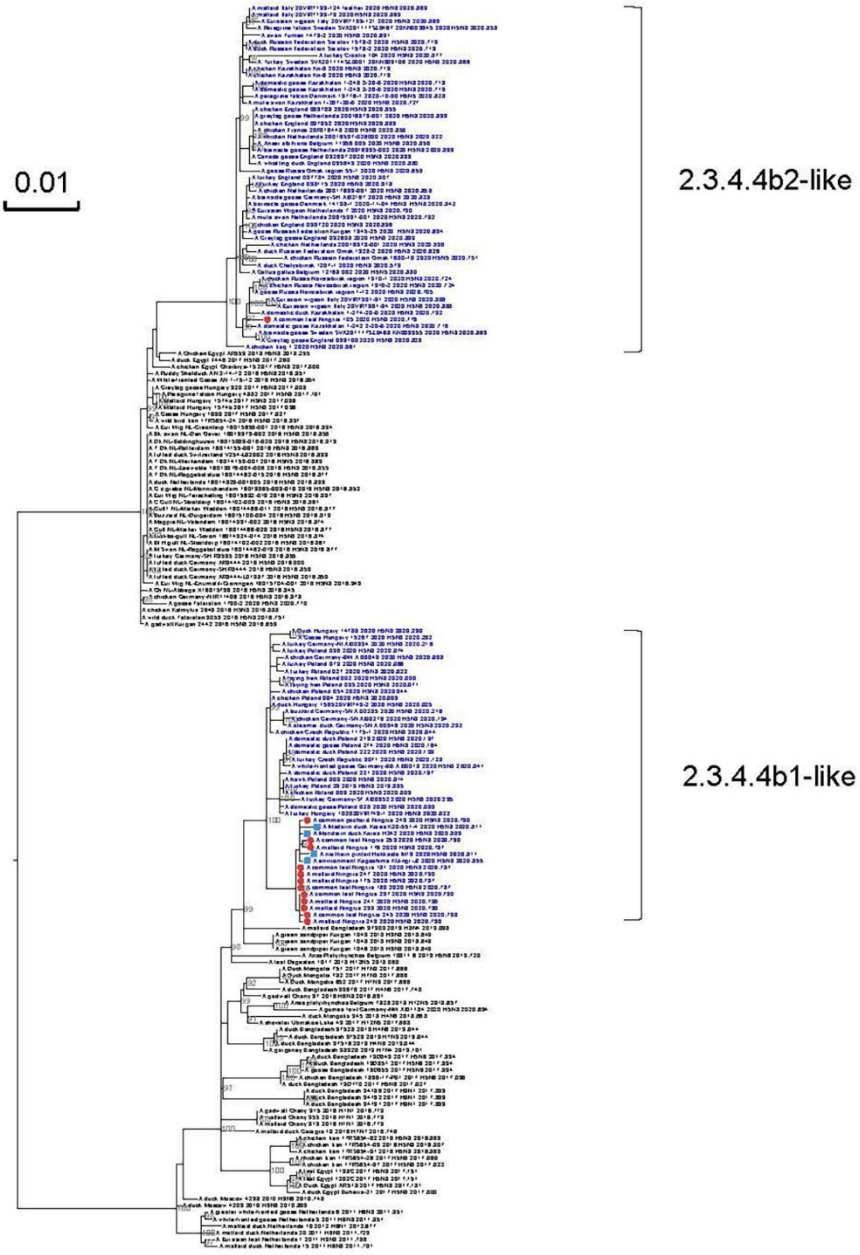

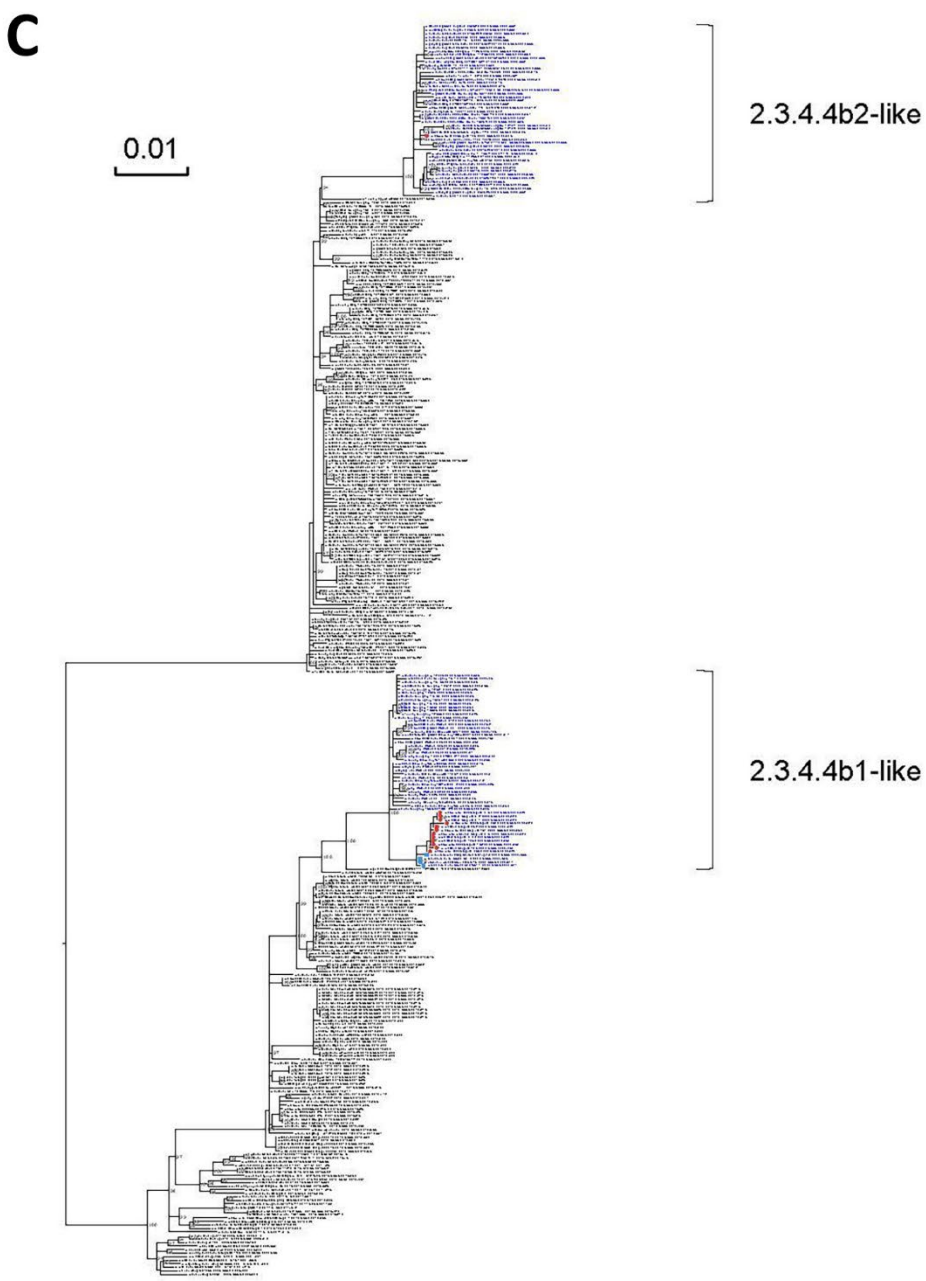
C
0.01
2.3.4.4b2-like
2.3.4.4b1-like

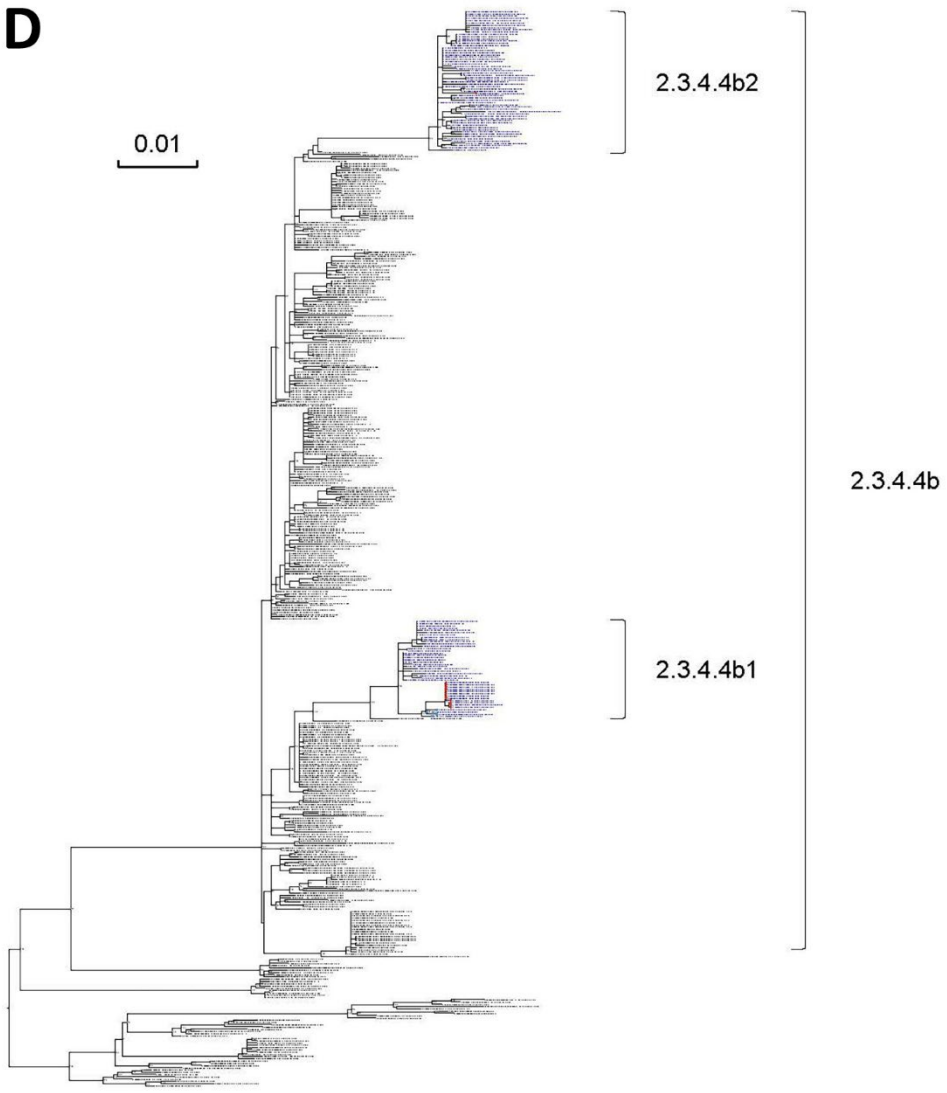
D
0.01
2.3.4.4b2
2.3.4.4b1
2.3.4.4b

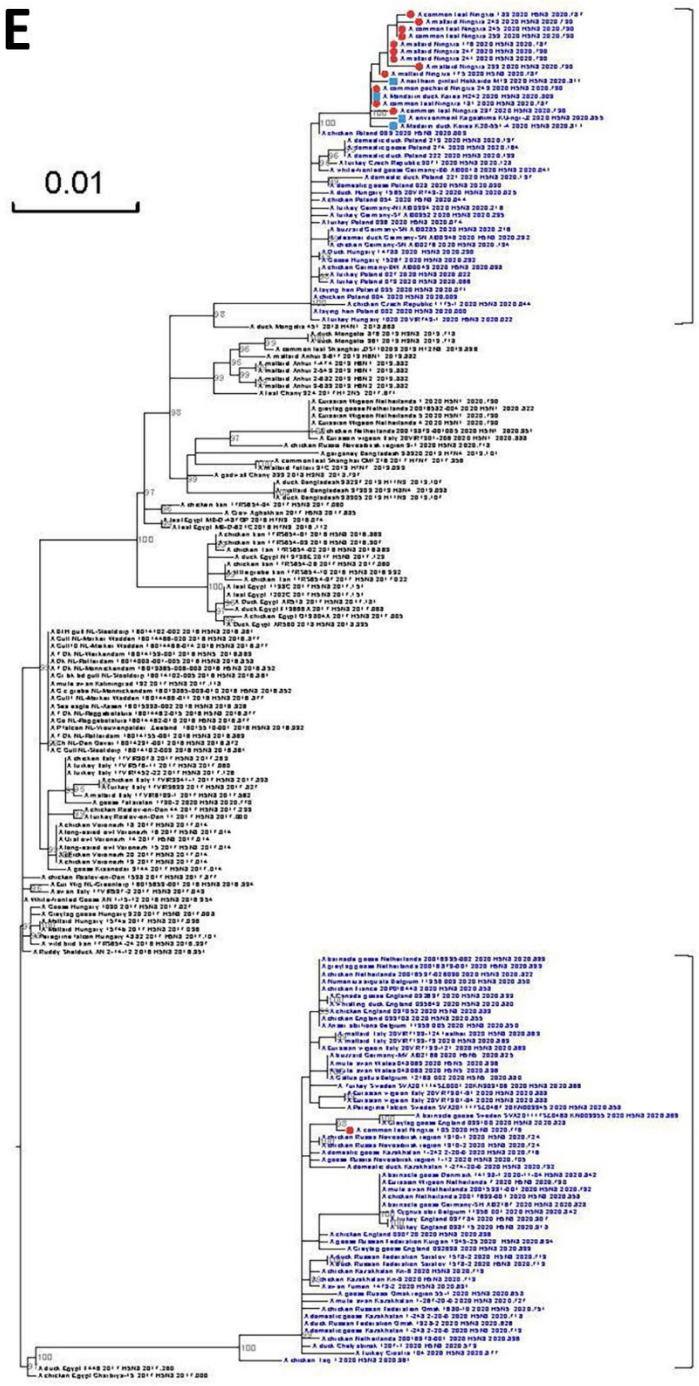
E
0.01
2.3.4.4b1-like
2.3.4.4b2-like

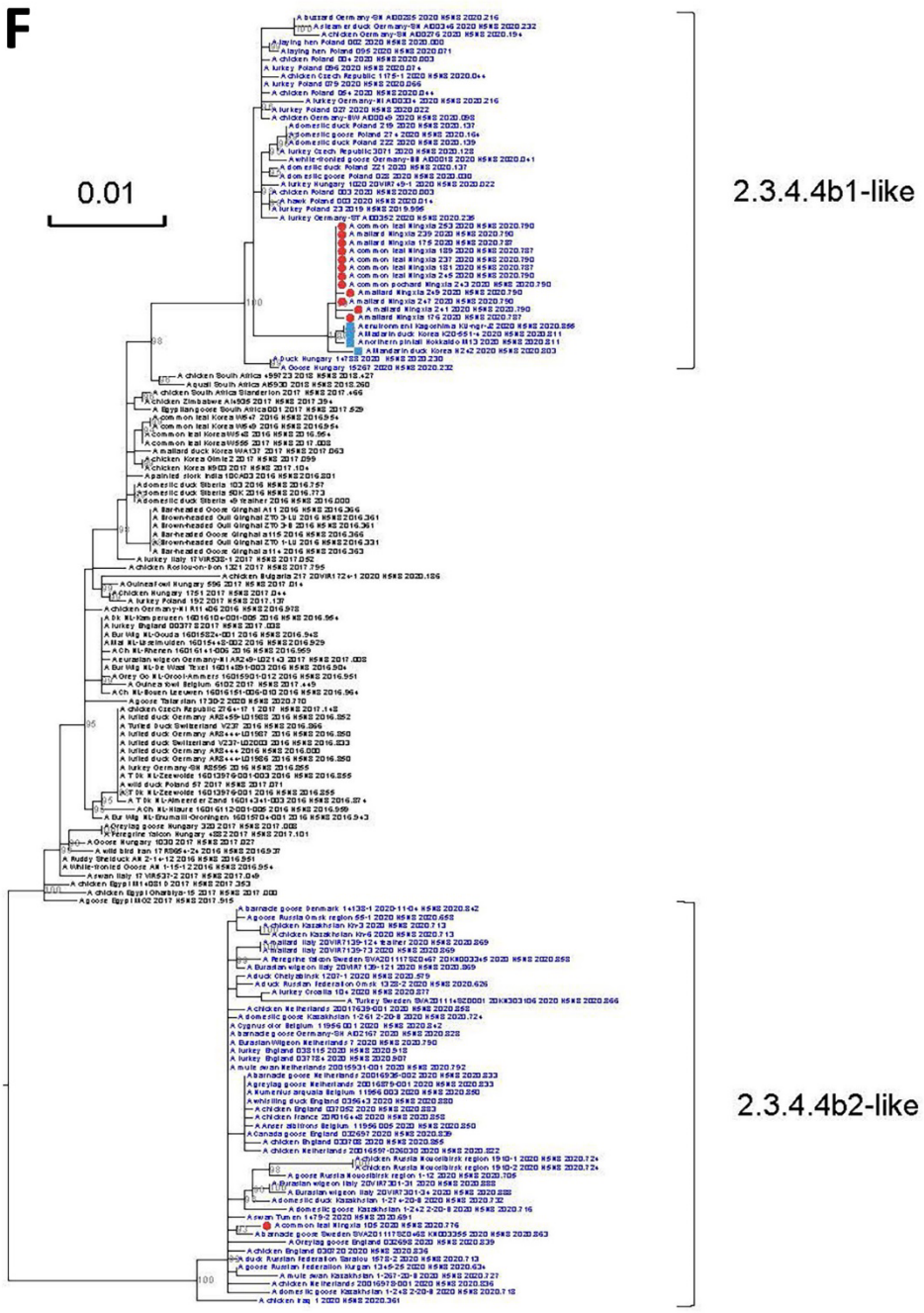
F
0.01
2.3.4.4b1-like
2.3.4.4b2-like

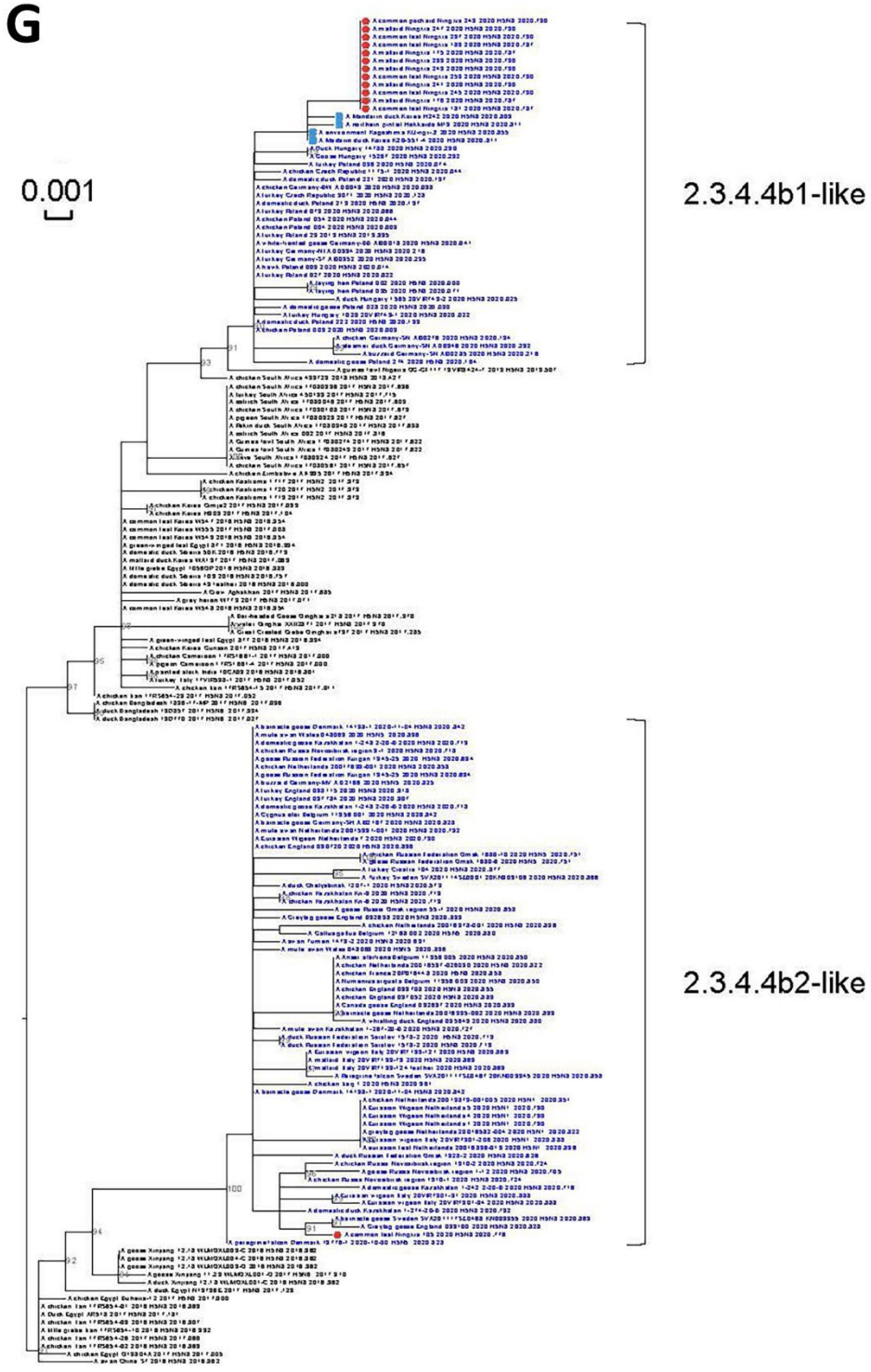
G
0.001
2.3.4.4b1-like
2.3.4.4b2-like

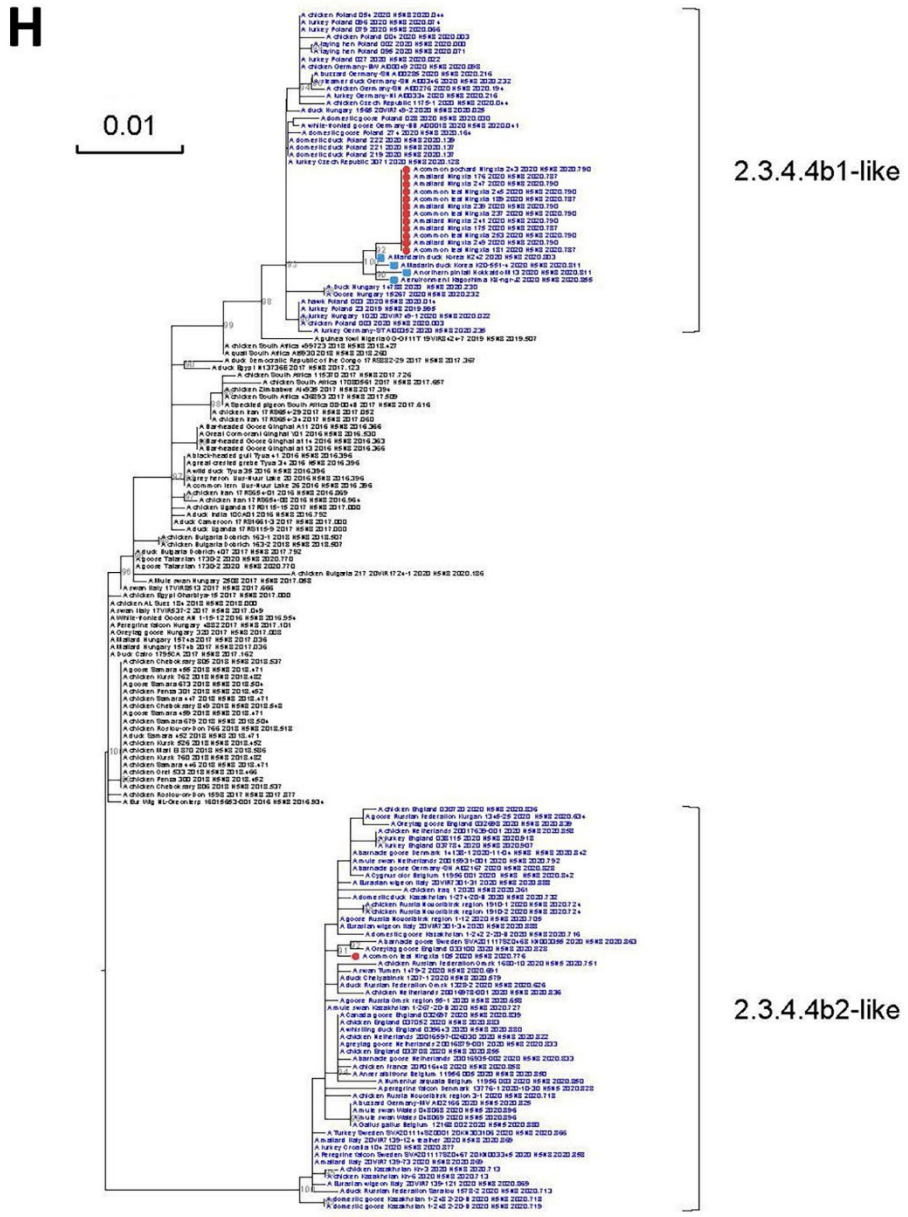

Appendix Figure 4. Maximum-likelihood phylogenetic trees. Our Ningxia H5N8 isolates are marked with red circles, the H5N8 viruses from South Korea and Japan isolated in October and November 2020 are marked with blue squares, and the clade 2.3.4.4b viruses isolated in 2020 are shown in blue. UFBoot support values >90 are shown. A) polymerase basic 2; B) polymerase basic 1; C) polymerase acidic; D) hemagglutinin; E) nucleoprotein; F) neuraminidase; G) matrix; H) nonstructural. Values along branches are bootstrap values. Scale bars indicate nucleotide substitutions per site.

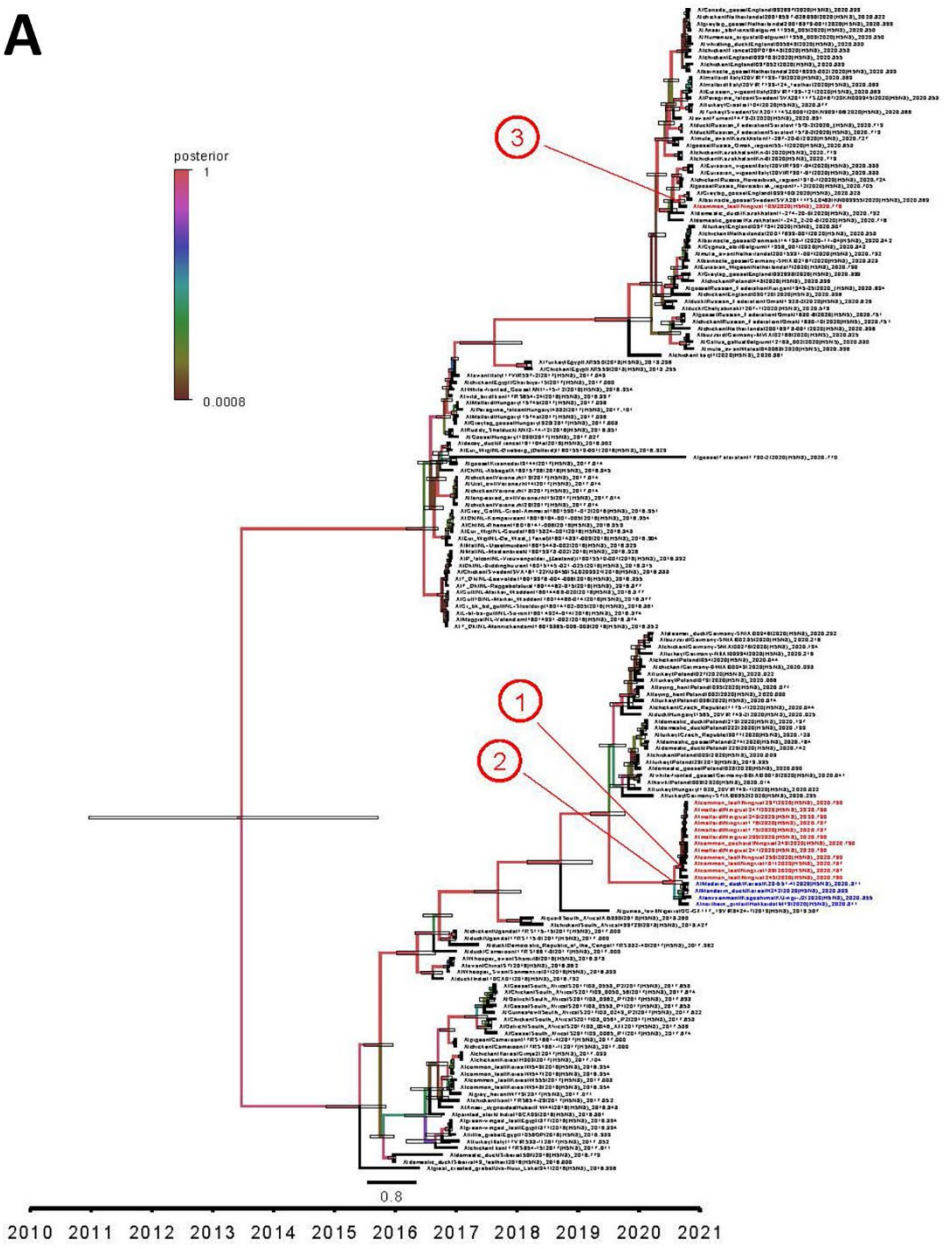
A
posterior
1
0.0008
3
1
2
0.8
2010
2011
2012
2013
2014
2015
2016
2017
2018
2019
2020
2021

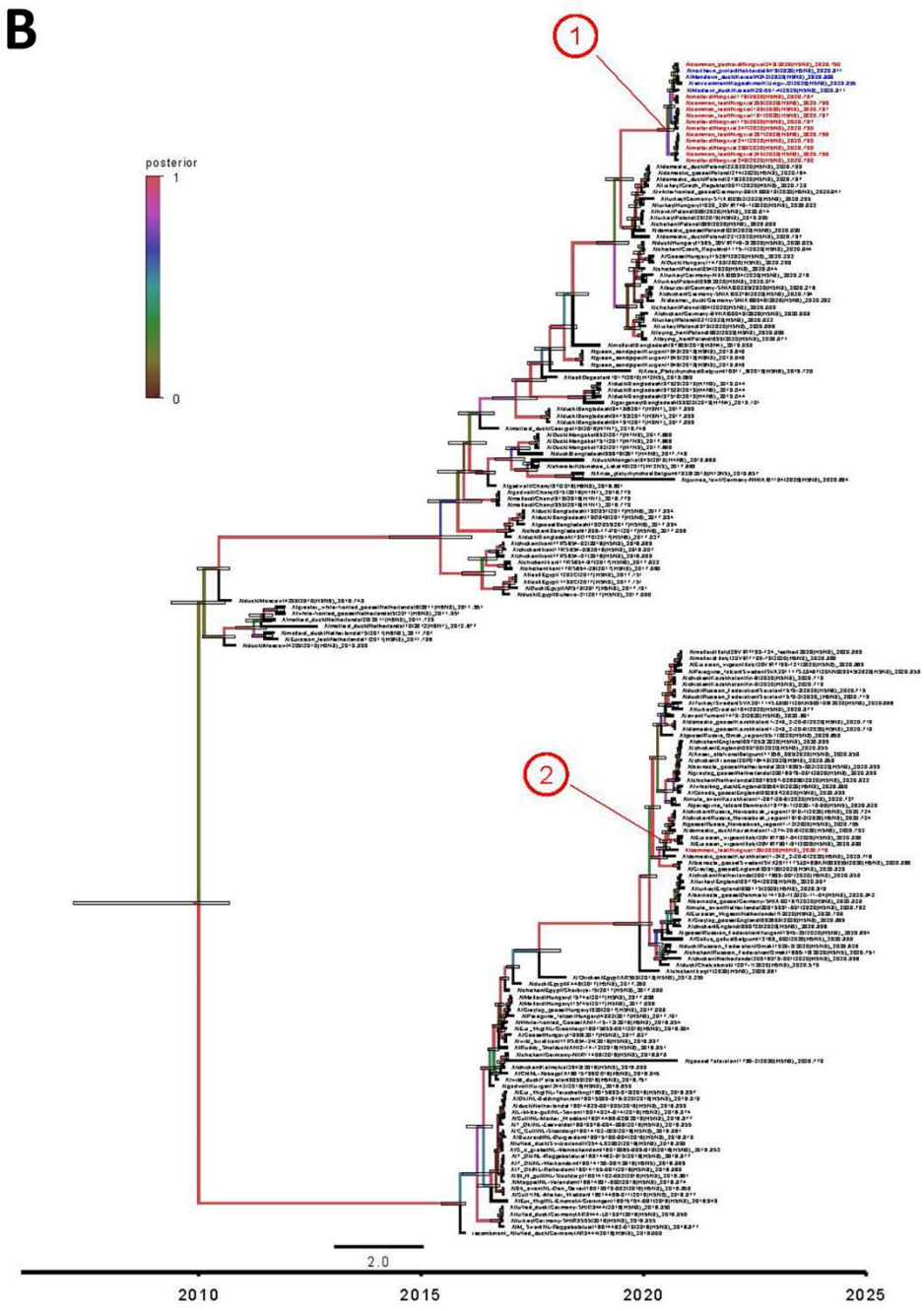
B
1
2
posterior
1
0
2.0
2010
2015
2020
2025

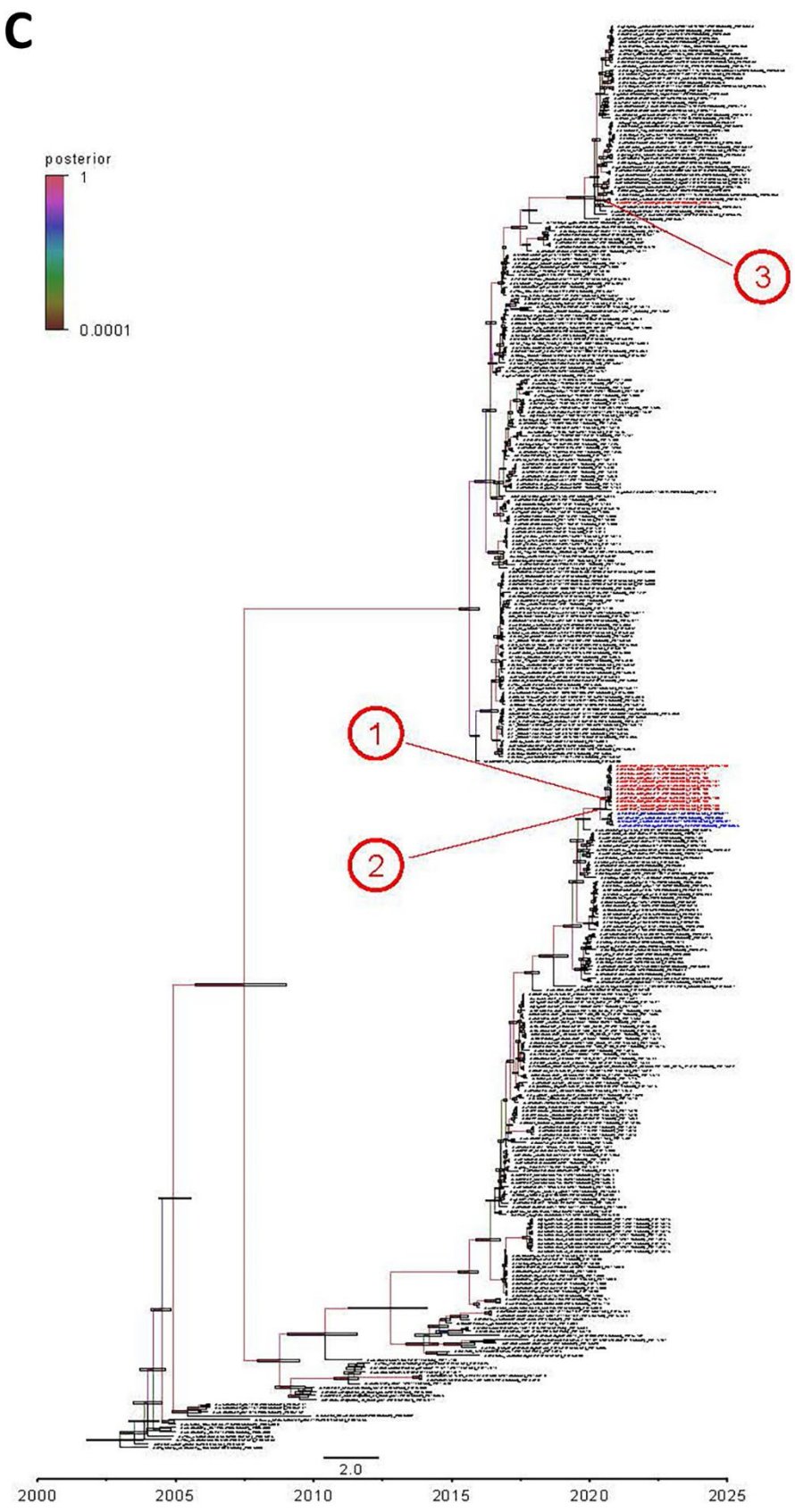
C
posterior
1
0.0001
1
2
3
2.0
2000
2005
2010
2015
2020
2025

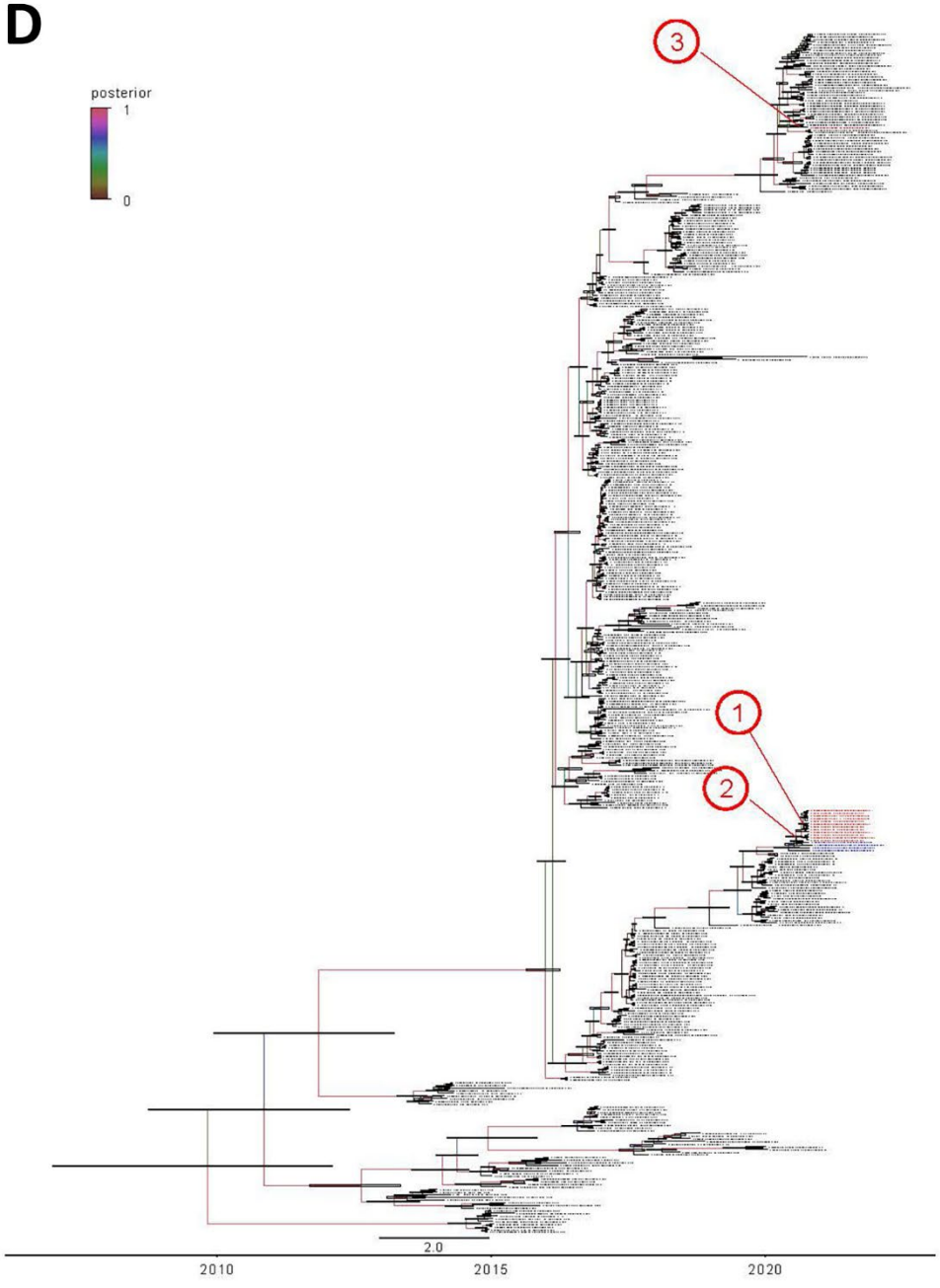
D
posterior
1
0
3
1
2
2.0
2010
2015
2020

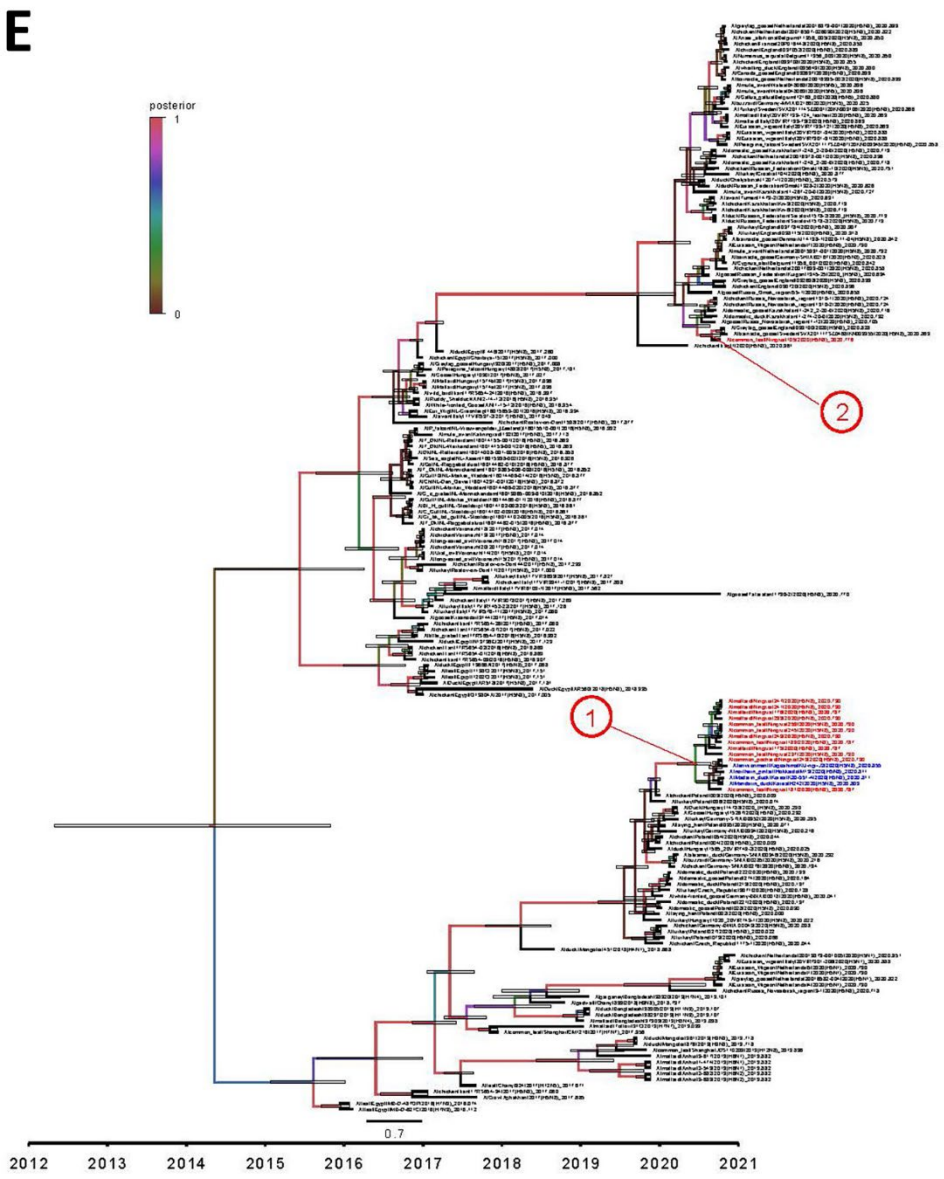
E
posterior
1
0
1
2
0.7
2012
2013
2014
2015
2016
2017
2018
2019
2020
2021

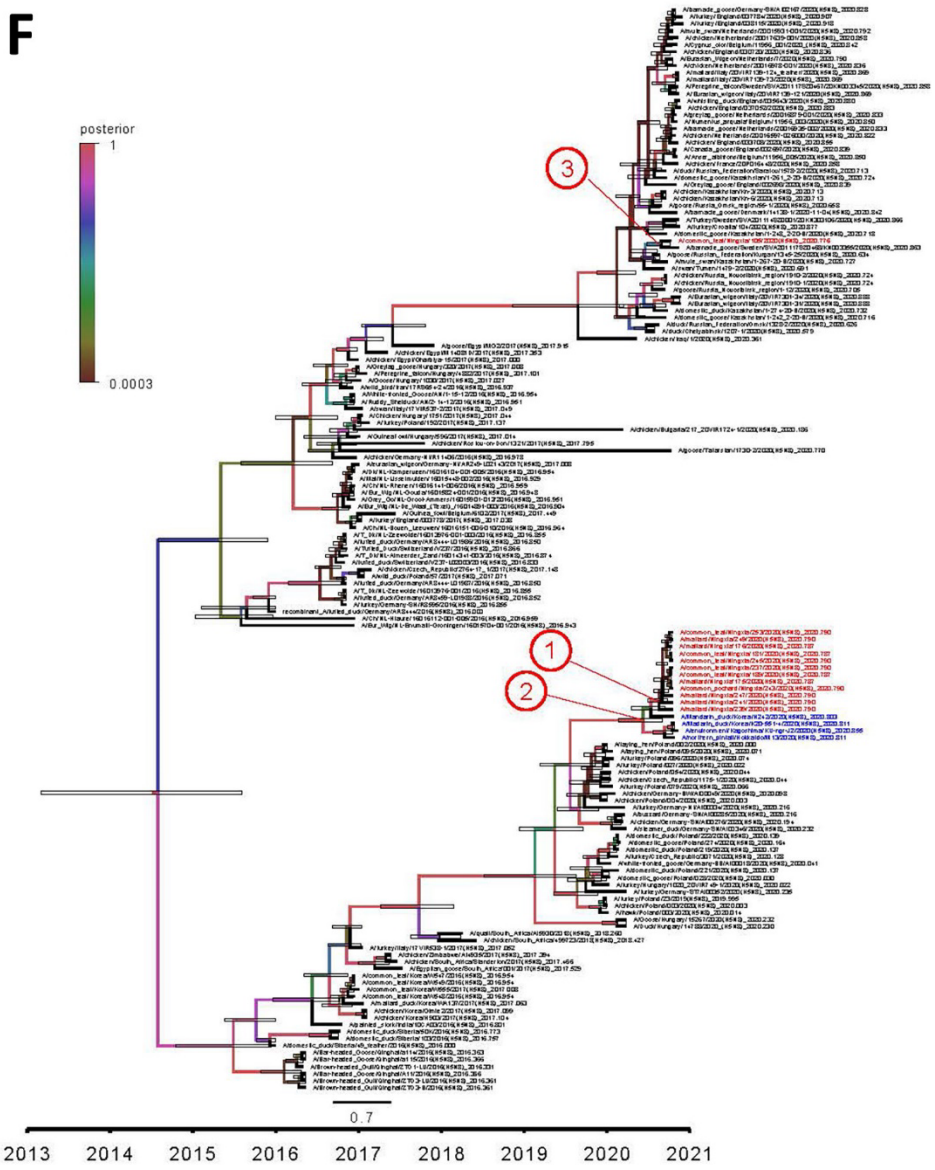
F
posterior
1
0.0003
3
1
2
0.7
2013
2014
2015
2016
2017
2018
2019
2020
2021

G

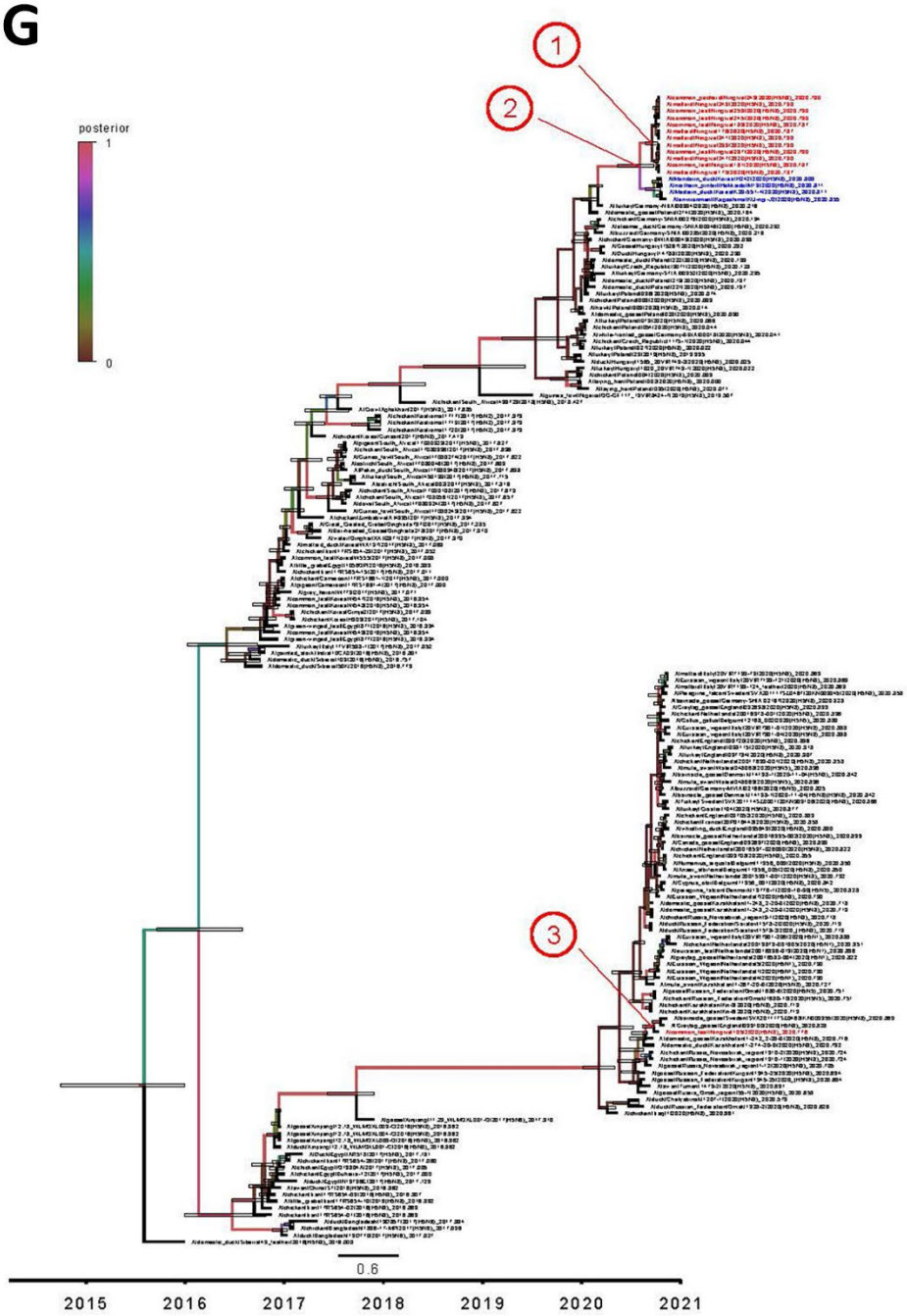

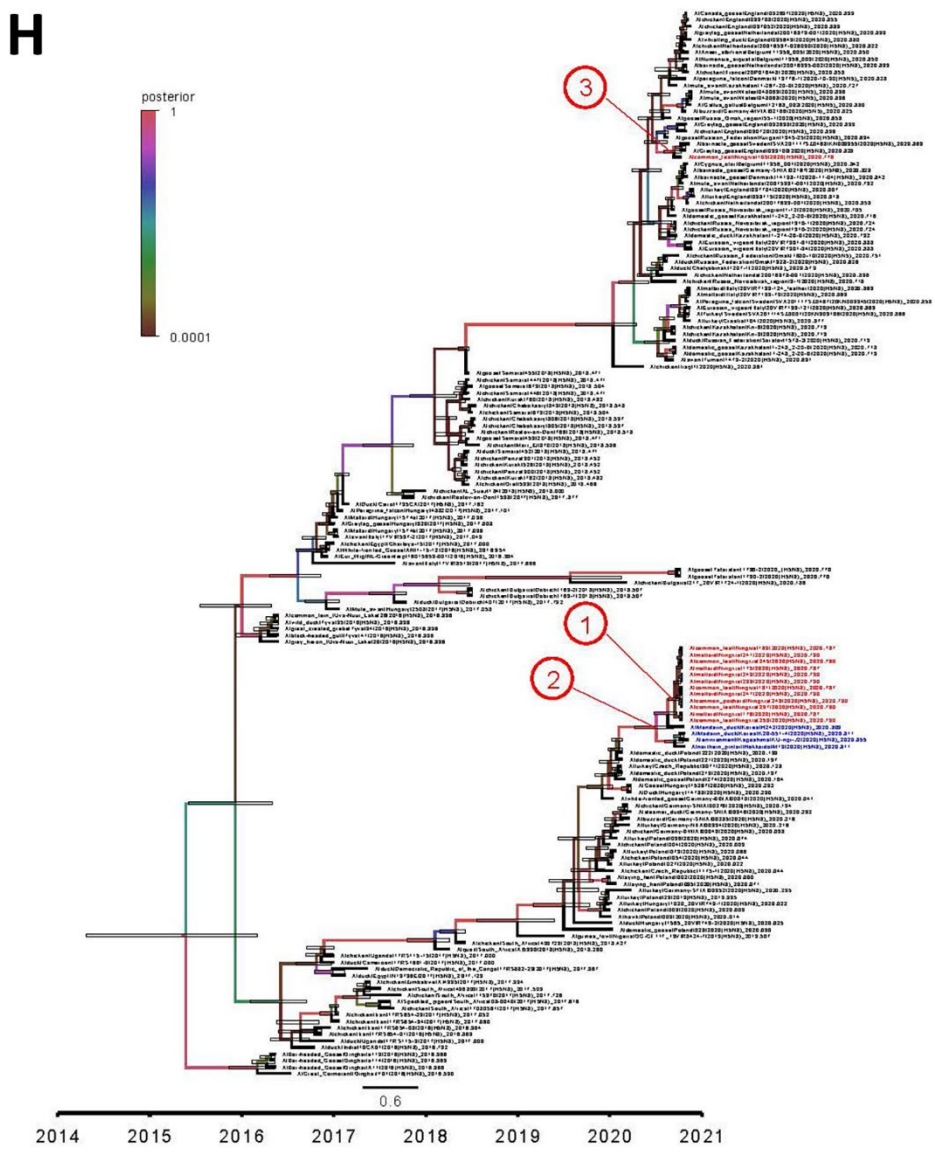

Appendix Figure 5. Maximum clade credibility phylogenetic trees (years on the horizontal axis) of each gene segment of the viruses associated with the H5N8 viruses isolated in Ningxia, October 2020. The Ningxia H5N8 isolates are shown in red, and the H5N8 viruses isolated in South Korea and Japan during October and November 2020 are shown in blue. The horizontal bars indicate the 95% highest posterior density (HPD) intervals of the most recent common ancestor. A) polymerase basic 2; B) polymerase basic 1; C) polymerase acidic; D) hemagglutinin; E) nucleoprotein; F) neuraminidase; G) matrix; H) nonstructural. Values along branches are bootstrap values. Scale bars indicate nucleotide substitutions per site.